Lab on a Chip

Cite this: *Lab Chip*, 2012, **12**, 647

www.rsc.org/loc

PAPER

Polymer-monovalent salt-induced DNA compaction studied *via* single-molecule microfluidic trapping

Weilin Xu* and Susan J. Muller

Received 14th September 2011, Accepted 28th November 2011
DOI: 10.1039/c2lc20880f

Polymer-monovalent salt-induced single-molecule DNA compaction/condensation in a microfluidic stagnation point flow was studied by analyzing both DNA compaction images and time trajectories. For the whole DNA compaction process we observed three successive steps: ***Step I***, a relaxation process of the stretched DNA that occurs slowly along the whole DNA chain, ***Step II***, nucleus formation and growth, and ***Step III***, corresponding to a rapid compaction of the chain. A memory effect was observed between ***Steps I*** and ***III***, and a new (intruder-induced) nucleation mode was observed for the first time. This study extends the use of the microfluidic stagnation point flow, which we have previously used for sequence detection and to measure enzyme kinetics site-specifically.

Introduction

Compaction or condensation of DNA, usually defined as the collapse of extended DNA chains into compact structures (such as rods, fibers, flexible rings, and toroids)[1] induced by multivalent metal cations,[2–4] polycations,[5–7] cationic lipids,[8,9] detergents,[6,10] peptides,[11] and a variety of noninteracting polymers,[12,13] has been extensively studied due to its importance in biology and artificial gene therapy systems. It has been challenging to study the effects of various parameters, such as solvent composition, temperature and concentrations of added chemicals or low molecular weight salts, on the speed or kinetics of DNA compaction.[14] For example, polyethylene glycol (PEG)-induced DNA compaction was discovered many years ago by Lerman *via* sedimentation studies.[13] The effect of low-molecular weight salt on the critical PEG concentration at the point of free DNA collapse has been predicted and observed,[14–16] but reports about the effect of low-molecular weight salts, especially monovalent salt on the PEG-induced (or polymer-salt-induced) DNA compaction kinetics are still rare.[15–19]

Herein we use a single molecule microfluidic trapping system to study the monovalent salt (NaCl) triggered PEG-induced single molecule DNA compaction process. We use NaCl since the monovalent cation Na^+ produces the fastest compaction compared with other alkali metal salts for PEG-induced DNA condensation in our experiments as well as in reports in the literature.[20–23]

It is well known that microfluidic stagnation point flows have a point of zero velocity at which a DNA molecule may be trapped and held using flow forces without tethering the DNA to a surface or otherwise modifying it. Near a stagnation point in the planar extensional flow generated in a microfluidic "cross-slot" (Fig. 1), hydrodynamic forces may then be used to linearize or alter the conformation of the DNA while holding it at a fixed point.[24–27] The steady-state extension of the DNA can be easily controlled through the flow strength, and near complete extension of DNA molecules has been achieved.[26] By flowing in solutions with different compositions through the opposing channels of the cross-slot, this single molecule microfluidic method was found to be suitable for a broad range of single-molecule studies. For example, we have recently demonstrated the use of such a flow to detect target sequences and examine the cleavage kinetics of restriction enzymes on DNA with or without

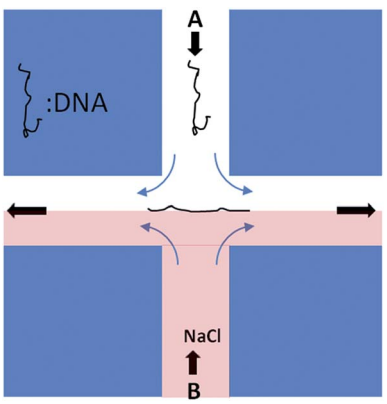

Fig. 1 The scheme for single molecule experiments with stagnation point flow, arrows show the flow directions in the cross-slot device. Individual DNA molecules flow in from channel A where they are trapped and stretched at the stagnation point. If there is extra NaCl flowing in from the opposite channel B, Na^+ will combine with the DNA molecule and induce its compaction which can be monitored by fluorescence microscopy.

Department of Chemical Engineering, University of California, Berkeley, Berkeley, CA, 94720, USA. E-mail: weilinxu@lbl.gov

fluorescent probes.[28–30] The ability to introduce the DNA through one inlet and rapidly linearize it and to introduce the salt through the opposing inlet, so that the DNA is exposed to salt only along the stagnation streamline, is crucial to the present study.

In the present case as shown in Fig. 1, individual YOYO-1 stained, double-stranded λ-bacteriophage DNA molecules in buffer containing a high concentration (25 wt%) of PEG of molecular weight 8 kDa flow in from channel A. The flow rate is chosen such that the DNA molecules enter the stagnation point and quickly stretch to near-full extension. Buffer without DNA but with PEG and excess NaCl flows in at the same flow rate from the opposite channel B. The extra Na^+ combines with the trapped DNA molecule and triggers PEG-induced DNA compaction which can be monitored *via* fluorescence microscopy by measuring the DNA length as a function of time. Thus, the effect of added NaCl on the PEG-induced DNA compaction kinetics can be studied systematically at the single molecule level, we believe for the first time.

Materials and methods

Single molecule assay

The 0.3 nM double-stranded λ DNA (New England Biolabs) in buffer (20 mM sodium phosphate, 100 mM NaCl and 1 M triethylene glycol (TEG), 100μg mL^{-1} bovine serum albumin, pH 7.3) was stained by adding 3.6 μL of 50 μM YOYO-1 (Invitrogen) and incubating in the dark overnight at room temperature, yielding a staining ratio of 4 : 1 (bp: YOYO-1).[30] Before single-molecule experiments, the above stained DNA was diluted to 1.0 pM DNA using H_2O (350μL), TEG (150μL), visualization buffer (500μL, 10mM sodium phosphate, 10 mM NaCl, and 1 M TEG, pH 7.3) and viscosified visualization buffer (1mL, 10mM sodium phosphate, 10 mM NaCl, and 25% PEG-8000, pH 7.3). Thirty minutes before starting single molecule experiments, 2 μL of 1000x glucose oxidase, 2 μL 1000x catalase and 20 μL BME were added to the above solution. As shown in Fig. 1, this DNA solution was directed, *via* a syringe pump (Harvard PHD2000), into one of the two inlet channels (channel A) of a microfluidic cross slot device, the condensation reagent NaCl solution, consisting of exactly the same buffer as the DNA solution without DNA but with additional NaCl at various concentrations, was flowed into the opposing inlet channel (channel B) using the same syringe pump and same flow rate. This creates a stagnation point at the channel intersection at which a DNA molecule may be trapped and stretched (see below). Movies visualizing the DNA were captured using a 100×, 1.4-NA oil-immersion objective on a fluorescence microscope (Leica) and a monochrome image-intensified, cooled CCD camera (Photometrics 512b) and SimplePCI software. Movies were analyzed with ImageJ software to get information about the DNA length change with time.

We note that the flow rates of the two streams A and B are held constant, and measurements start whenever a DNA molecule enters the stagnation point and is trapped. As a result, the PEG and NaCl concentration fields in the cross-slot are stationary. From experiments with small fluorophores and scaling arguments, the spatial scale over which diffusion leads to the blurring of the interface between streams A and B (and the two streams becoming homogeneous in NaCl concentration) is of order $V_o w^2/D$, where V_o is a characteristic velocity in the channel, w is the channel half-width, and D is the diffusivity of NaCl in the buffer. For our system, this is of order 40 cm; that is, the spatial variations in NaCl concentration over the length scale of the stretched DNA (~20 microns), are negligible. Since the experiment starts when a DNA molecule flowing with the upper stream A reaches the stagnation streamline, the time scale over which the DNA experiences concentration changes are the convection time scale L/V_o (where L is the length of the stretched DNA molecule), which is of order 0.04 s in our system. This time scale is much shorter than the time scale over which we report changes in length due to compaction.

Cross slot preparation

Microfluidic cross slots with channel widths of 800 μm and inlet lengths of 3 mm were prepared using standard soft lithography techniques.[35] Device masters were fabricated to a 130-μm depth using SU-8 2100 resist (MicroChem). PDMS (Sylgard 184, Dow Corning) molds were cast from the master, and inlets and outlets were created using a 16-gauge blunt-tipped needle. Molds were sealed to glass coverslips after treatment with oxygen plasma. Microbore tubing (Tygon, 0.02″ID) was seated directly into the inlet and outlet holes, providing a water-tight seal. Prior to each experiment, tubing and interior surfaces of the sealed microfluidic device were treated for 10 min at room temperature with isopropyl alcohol and subsequently rinsed with ultrapure (18 MΩ) water. This reduced the incidence of trapped air bubbles during channel loading. Next, the tubing and device were incubated for 10 min with 10 mg ml^{-1} BSA in PBS buffer (100 mM sodium phosphate, 1.37 mM NaCl, 27 mM KCl, pH 7.4), which helps to reduce surface adsorption of the fluorescent molecules. BSA was rinsed out of the device using ultrapure water. Immediately before experiments, the tubing and microfluidic device were first primed by loading viscosified visualization buffer into the device. Following experiments, devices were flushed thoroughly with water. Each device consists of two channels that intersect at right angles, channel dimensions were 130μm in depth and 800 μm in width. The flow rate in all studies was held constant at 80μL per hour. The two fluid streams meet at the channel intersection and flow out through the two channels at 90° to the inlet channels (see Fig. 1). This creates a stagnation point at the channel intersection where DNA molecule may be trapped and linearized by the extensional flow generated along the outlet axis. Indeed, the degree of linearization can be easily controlled by varying the flow rate.[26]

Results & discussion

In numerous previous studies,[26,27,29,32] individual DNA molecules in buffers viscosified with sucrose have been stretched and held for tens of minutes or longer with no evidence of compaction. That is, the length of individual DNA molecules, once trapped and stretched, remained constant as long as they remained trapped at the stagnation point. As part of the present study, a series of control experiments were performed to confirm that the DNA compaction process was induced by the combination of PEG and salt. First, PEG, in the absence of NaCl, was

substituted for sucrose as the viscosifying agent in the buffer, and no compaction of DNA was observed. In a second set of control experiments, increasing concentrations of NaCl or KCl were added to the sucrose-viscosified buffer solutions in the absence of PEG. Even at saturated NaCl or KCl concentrations, no DNA compaction was observed in the absence of PEG: the length of individual, stretched DNA molecules remained constant as long as they remained trapped at the stagnation point. Thus both PEG and NaCl are required to effect changes in the length of the trapped DNA; this is consistent with previous reports of polymer-salt-induced DNA compaction.[13,20]

Fig. 2(a) shows a sample λ DNA molecule changing conformation at the stagnation point throughout the compaction process. The DNA molecule enters the stagnation point and quickly (within a few tens of milliseconds) stretches to near-full extension. On reaching the stagnation point, it is exposed to NaCl in the opposing stream, and begins compacting. Fig. 2(b) is a typical compaction time trajectory obtained from such a movie for another λ DNA molecule. The inset in Fig. 2(b) shows four images of this DNA molecule at different times labeled from **1** to **4**. They show three successive steps for DNA compaction. ***Step I***, a slow relaxation process of extended DNA molecules,[31] occurs along the whole DNA chain (from **1** to **2**). After the DNA is sufficiently relaxed, at the end of ***Step I*** nucleation and growth occurs gradually (***Step II***) by DNA (in the case shown) folding at one end (evidenced by the bright point appearing at the right end in **3**).[2,32] Subsequently, the growth of the nucleus occurs quickly (***Step III***) as the nucleated end incorporates DNA from the chain and finally forms a compact structure (a single bright point in **4**). The observation of these successive steps is consistent with Baumann's conclusion that "…intramolecular condensation can occur only when the DNA is sufficiently relaxed that intramolecular loops can occur, providing strong support for a lateral interaction rather than an elastic buckling mechanism."[33]

Previously Yoshikawa *et al.* reported ***Step II*** and ***III*** by observing the free DNA nucleation and growth in quiescent, aqueous solution with the addition of PEG.[14,19] No initial relaxation step (***Step I***) was observed because the DNA is already relaxed in free solution. That is, at low extension of DNA, the intramolecular loops can occur easily without further relaxation, while in our experiments, the DNA molecules were almost fully extended,[28–30,34] so the DNA chains need to relaxation sufficiently (***Step I***) before nucleation (intramolecular loop formation) can occur.[5,28,33] Theoretical work by Lee and Thirumalai on the collapse of free flexible polyampholytes by counterions predicts a two-step process.[35] The initial step is the formation of pearl-necklace structures and the second step is the merging (or growth) of these pearl-necklace domains to form a compact globular structure. These two steps correspond to ***Step II*** and ***III*** in our case, respectively. Again, no relaxation step is predicted because only the collapse of free DNA without extension was considered. Brewer *et al.*, in a study of salt-induced DNA condensation in the absence of PEG, also observed only ***Steps II*** and ***III*** in experiments in which they trapped one end of DNA molecules stretched by flow. We believe the reasons these researchers did not observe and report a rate for ***Step I*** may be attributed to both the lower degree of stretching of the DNA (<63%) and the use of a much less viscous solvent. In our studies, the highly viscous solvent slows the initial relaxation dynamics and makes the process easily observable. With force-microscopy Ran *et al.* obtained similar DNA compaction time trajectories to ours shown in Fig. 2b, but ***Step I*** could not be discriminated from ***Step II*** since they were not directly visualizing the DNA backbone in their experiments.[36]

From the whole trajectory point of view as shown in Fig. 2b, both ***Step I*** and ***Step III*** can be approximated as linear in time. For the nucleus growth (***Step III***) this linear relationship is consistent with previous observations[5,14] and theoretical predictions.[35,37] The linear relationship also means that for each DNA molecule the compaction rates for these two steps are constant during the whole process. By linear-fitting, for example, as shown in Fig. 2b (dotted lines), $V_I = 1.3$ μm s^{-1} and $V_{III} = 25$ μm s^{-1} were obtained for these two linear processes. In ***Step III*** we cannot tell whether ***Step I*** is still progressing or not, but since in most cases V_{III} is much larger than V_I, for simplicity we assume the rate for nucleus growth to be V_{III}.

Two dimensional (2D) histograms of V_I–V_{III} are shown in Fig. 3 for more than 1000 DNA molecules, reflecting the ensemble average of a single-molecule memory property.[38] There

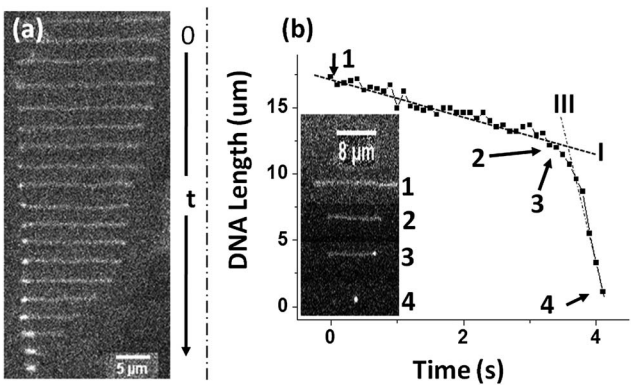

Fig. 2 (a) Images of DNA molecular configurations with uniform time interval (0.3 s) to show DNA compaction process after binding with Na^+ at the stagnation point. In this experiment, DNA enters one channel and is trapped at a point; [NaCl] = 0.16 M flows in from the opposite direction. (b) A typical compaction time trajectory for a λ DNA molecule, the inset is four images of DNA at different times labeled **1** to **4**. The two straight lines are linear fits of ***Step I*** and ***Step III***.

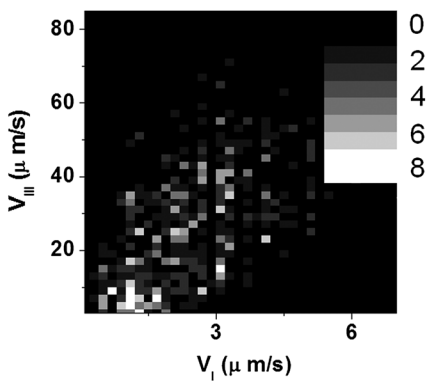

Fig. 3 2D distribution for a pairs of ***VI*∼*VIII*** for more than 1000 DNA molecules obtained for varying NaCl concentrations.

is a diagonal feature, indicating that a small V_I tends to be followed by a small V_{III}, and a large V_I tends to be followed by a large V_{III}. The correlation coefficient between these two rates was 0.6, also indicating a significant memory effect in the stretched DNA compaction process. The reason of this correlation in the rates V_I and V_{III}, reported here for the first time, is at present unknown.

For ***Steps II*** and ***III***, we observed three different dynamic behaviors from compaction movies. Specifically, Fig. 4(a) shows nucleation at one end of the DNA, after which the compact structure grows rapidly by dragging the remaining part of the coil toward the nucleated center.[5] This nucleation mode is also shown in Fig. 2(a). Fig. 4(b) shows nucleation occurring at a random point between the two ends of the DNA,[33] subsequently, the nucleus grows with different rates at the two ends and a second nucleation site appears late in the process.[35,39] Fig. 4(c) shows the binding of a large "intruder" (here possibly a compacted DNA fragment) on DNA can trigger nucleation. Although the mechanism for this nucleation process is not clear, the encapsulation of the intruder by DNA compaction may be a good candidate as a delivery vehicle in gene therapy.[40,41] Our experiments indicate that more than 90% of the nucleation centers observed here for DNA compaction are located at either end of the DNA chain. This is consistent with previous observations and theoretical predictions of DNA compaction in free solution.[42] It is also consistent with Baumann's observation that the free polymer ends are not absolutely required for DNA collapse.[33]

Based on these observations, we sketch a mechanism for the whole compaction process of a fully stretched DNA molecule in extensional flow induced by both PEG and salt, as shown in Fig. 4(d). Salt binds to the extended DNA chain, decreasing the persistence length and the effective relaxation time of the chain. Makita *et al.*[23] used single molecule visualization measurements to determine the effect of NaCl concentration, [NaCl], on persistence length p, and reported the persistence length varies with salt concentration as $p \sim A + B[NaCl]^{-0.493}$, where A and B are constants. The relaxation time depends strongly on persistence length, for example, in the Zimm model,[45] the relaxation time scales as p^3. Thus, a relatively small increase in salt concentration will result in a significant decrease in relaxation time. At the fixed volumetric flow rate used in the experiments, this decreased relaxation time results in a lower effective flow strength for the chain, and the DNA becomes less stretched. If there were no extra salt-binding on the stretched DNA, the shrinkage or compaction would not happen even with a high concentration of PEG present,[28–30] as confirmed in our control experiments. After the binding of a suitable amount of extra salt (compaction cofactor), the DNA relaxes (***Step I***).[31] This relaxation allows nucleation to happen easily by DNA folding at either end, at any region between the two ends, or even by the binding of an external impurity. Once the nucleus forms (***Step II***), it grows rapidly by consuming the remaining part of the DNA coil and finally forms a compact structure (***Step III***).[2,43]

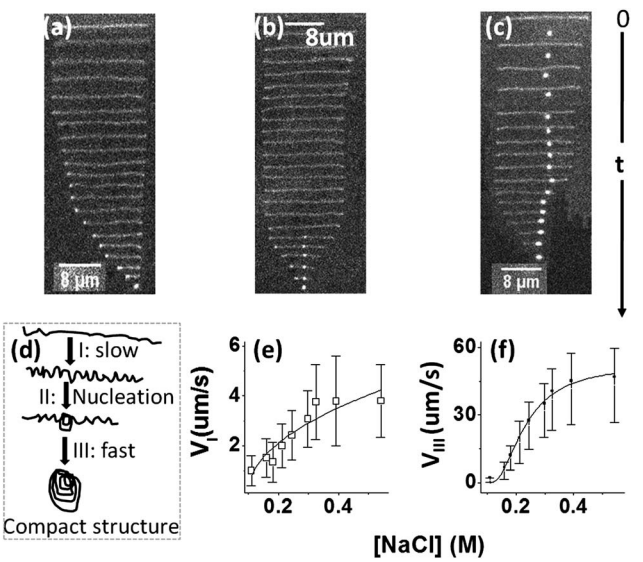

Fig. 4 (a) DNA nucleates at either of two ends; (b) nucleation occurs at any point between the two ends; (c) nucleation triggered by binding of an intruder; (d) Model for stretched DNA compaction; (e) Salt concentration titration of V_I, solid line is the empirical fitting curve; (f) Salt concentration titration of V_{III}, solid line is the empirical fitting curve. The error bars in (e) and (f) are standard deviations over multiple measurements.

Experiments conducted at different NaCl concentrations showed that the rates of both ***Step I*** and ***Step III*** were limited by the rate of Na^+ binding to the DNA molecule (Fig. 4e and 4f). At low salt concentrations, the rates vary approximately linearly, which is consistent with previous single molecule observations,[5] but when the salt concentration increases, both of these rates saturate gradually. To the best of our knowledge, this is the first observation of the saturation behavior of the compaction rates.

In summary, we have used a microfluidic stagnation point device to study the polymer (PEG)-salt (NaCl)-induced single-molecule DNA compaction kinetics. The microfluidic device allows trapping and extension of the DNA chain by flow forces without surface tethering; using double-stranded DNA that has been fluorescently labeled with YOYO-1, we can directly observe real-time changes in the chain conformation on exposure to salt at the stagnation point. We observed three successive steps: ***Step I***, a relaxation process of the stretched DNA, occurs along the whole DNA chain *via* the low-molecular weight salt binding, ***Step II*** is nucleation of a compact structure followed by its rapid growth in ***Step III***. For fully stretched DNA molecules, ***Step I*** is required for the occurrence of ***Steps II*** and ***III***. A memory effect was observed between ***Steps I*** and ***III***, and is reported here for the first time. Three different nucleation modes were observed, including one (intruder induced nucleation) that has not been previously reported. Finally, we note that this is a new application of a microfluidic stagnation point tool that we have used previously for target sequence detection and measurements of enzyme kinetics,[28,29] and we anticipate that the technique will be useful for a broad range of single molecule kinetics studies.

Acknowledgements

This work was funded by NIH award R21HG004342. The authors would also like to acknowledge Rebecca Dylla-Spears, who fabricated the microfluidic devices and Hagar Zohar, who supplied the sucrose buffer without PEG.

References

1 V. B. Teif and K. Bohinc, *Prog. Biophys. Mol. Biol.*, 2011, **105**, 208–222.
2 W. Fu, X. Wang, X. Zhang, S. Ran, J. Yan and M. Li, *J. Am. Chem. Soc.*, 2006, **128**, 15040–15041.
3 J. Widom and R. L. Baldwin, *Biopolymers*, 1983, **22**, 1595–1620.
4 P. G. Arscott, C. Ma, J. R. Wenner and V. A. Bloomfield, *Biopolymers*, 1995, **36**, 345–364.
5 L. R. Brewer, M. Corzett and R. Balhorn, *Science*, 1999, **286**, 120–123.
6 G. Krishnamoorthy, G. Duportail and Y. Mély, *Biochemistry*, 2002, **41**, 15277–15287.
7 D. K. Chattoraj, L. C. Gosule and J. A. Schellman, *J. Mol. Biol.*, 1978, **121**, 327–337.
8 A. D. Miller, *Angew. Chem., Int. Ed.*, 1998, **37**, 1768–1785.
9 Y. S. Tarahovsky, V. A. Rakhmanova, R. M. Epand and R. C. MacDonald, *Biophys. J.*, 2002, **82**, 264–273.
10 S. M. Mel'nikov, V. G. Sergeyev, Y. S. Mel'nikova and K. Yoshikawa, *J. Chem. Soc., Faraday Trans.*, 1997, **93**, 283–288.
11 G. Krishnamoorthy, B. Roques, J.-L. Darlix and Y. Mély, *Nucleic Acids Res.*, 2003, **31**, 5425–5432.
12 M. H. Kombrabail and G. Krishnamoorthy, *J. Fluoresc.*, 2005, **15**, 741–747.
13 L. S. Lerman, *Proc. Natl. Acad. Sci. U. S. A.*, 1971, **68**, 1886–1890.
14 K. Yoshikawa and Y. Matsuzawa, *J. Am. Chem. Soc.*, 1996, **118**, 929–930.
15 V. V. Vasilevskaya, A. R. Khokhlov, Y. Matsuzawa and K. Yoshikawa, *J. Chem. Phys.*, 1995, **102**, 6595–6602.
16 H. Kawakita, T. Uneyama, M. Kojima, K. Morishima, Y. Masubuchi and H. Watanabe, *J. Chem. Phys.*, 2009, **131**, 094901–094909.
17 J. E. B. Ramos, R. de Vries and J. R. Neto, *J. Phys. Chem. B*, 2005, **109**, 23661–23665.
18 K. Minagawa, Y. Matsuzawa, K. Yoshikawa, A. R. Khokhlov and M. Doi, *Biopolymers*, 1994, **34**, 555–558.
19 K. Yoshikawa and Y. Matsuzawa, *Phys. D*, 1995, **84**, 220–227.
20 A. A. Zinchenko and K. Yoshikawa, *Biophys. J.*, 2005, **88**, 4118–4123.
21 B. Luan and A. Aksimentiev, *J. Am. Chem. Soc.*, 2008, **130**, 15754–15755.
22 A. Savelyev and G. A. Papoian, *J. Am. Chem. Soc.*, 2006, **128**, 14506–14518.
23 N. Makita, M. Ullner and K. Yoshikawa, *Macromolecules*, 2006, **39**, 6200–6206.
24 D. Roulland-Dussoix, R. Yoshimori, P. Greene, M. Betlach, H. M. Goodman and H. W. Boyer, presented in part at the American Society for Microbiology, Conference on Bacterial Plasmids, Washington, D.C., 1974.
25 M. M. Horvath, J. Choi, Y. Kim, P. Wilkosz and J. M. Rosenberg, *Rebase Ref.*, 1999, 5897.
26 T. T. Perkins, D. E. Smith and S. Chu, *Science*, 1997, **276**, 2016–2021.
27 R. G. Larson, T. T. Perkins, D. E. Smith and S. Chu, *Phys. Rev. E: Stat. Phys., Plasmas, Fluids, Relat. Interdiscip. Top.*, 1997, **55**, 1794–1797.
28 W. Xu and S. Muller, *Lab Chip*, 2011, **11**, 435–442.
29 R. Dylla-Spears, J. E. Townsend, L. Jen-Jacobson, L. L. Sohn and S. J. Muller, *Lab Chip*, 2010, **10**, 1543–1549.
30 R. Dylla-Spears, J. E. Townsend, L. L. Sohn, L. Jen-Jacobson and S. J. Muller, *Anal. Chem.*, 2009, **81**, 10049–10054.
31 T. T. Perkins, S. R. Quake, D. E. Smith and S. Chu, *Science*, 1994, **264**, 822–826.
32 Y. Fang and J. H. Hoh, *J. Am. Chem. Soc.*, 1998, **120**, 8903–8909.
33 C. G. Baumann, V. A. Bloomfield, S. B. Smith, C. Bustamante, M. D. Wang and S. M. Block, *Biophys. J.*, 2000, **78**, 1965–1978.
34 V. Namasivayam, R. G. Larson, D. T. Burke and M. A. Burns, *Anal. Chem.*, 2003, **75**, 4188–4194.
35 N. Lee and D. Thirumalai, *J. Chem. Phys.*, 2000, **113**, 5126–5129.
36 S. Ran, X. Wang, W. Fu, Z. Lai, W. Wang, X. Liu, Z. Mai and M. Li, *Chin. Phys. Lett.*, 2006, **23**, 504–507.
37 B. Ostrovsky and Y. Bar-Yam, *Biophys. J.*, 1995, **68**, 1694–1698.
38 H. P. Lu, L. Y. Xun and X. S. Xie, *Science*, 1998, **282**, 1877–1882.
39 B. van den Broek, M. C. Noom, J. van Mameren, C. Battle, F. C. Mackintosh and G. J. L. Wuite, *Biophys. J.*, 2010, **98**, 1902–1910.
40 R. I. Mahato, Y. Takakura and M. Hashida, *Crit. Rev. Ther. Drug Carrier Syst.*, 1997, **14**, 133–172.
41 V. Vijayanathan, T. Thomas and T. J. Thomas, *Biochemistry*, 2002, **41**, 14085–14094.
42 Y. Matsuzawa, Y. Yonezawa and K. Yoshikawa, *Biochem. Biophys. Res. Commun.*, 1996, **225**, 796–800.
43 K. Besteman, S. Hage, N. H. Dekker and S. G. Lemay, *Phys. Rev. Lett.*, 2007, **98**, 058103–058106.